Available online at www.sciencedirect.com
SCIENCE DIRECT®
Journal of Chromatography A, 996 (2003) 33–43
JOURNAL OF CHROMATOGRAPHY A
www.elsevier.com/locate/chroma

Fractal calibration in size-exclusion chromatography I. An introduction

Rosa García-Lopera[a], Isabel Irurzun[b,1], Concepción Abad[c], Agustín Campos[a,*]

[a]*Departament de Química Física and Institut de Ciéncia dels Materials, Universitat de València, E-46100 Burjassot, València, Spain*
[b]*Departamento de Física, Universidad de Buenos Aires, Ciudad de Buenos Aires, República Argentina*
[c]*Departament de Bioquímica i Biologia Molecular, Universitat de València, València, Spain*

Received 17 October 2002; received in revised form 2 January 2003; accepted 1 April 2003

Abstract

The elution behaviour of different polymer–solvent systems in three types of organic columns for SEC has been compared and interpreted. The experimental data show that the classical universal calibration is not accomplished. Deviations from a unique curve are observed due to the binary and ternary interactions between the components of the system (solvent, polymer and gel) which results on secondary mechanisms accompanying the main pure or ''ideal'' SEC separation mechanism. Both, enthalpic and entropic effects are interpreted in terms of the swelling and crosslinking degrees of the gel packings, and are also related with the fractal characteristics of their surfaces, such as the fractal dimension and the available pore size. Moreover, a relationship between the fractal dimension of the pore surface and the chromatographic distribution coefficient is proposed.

Keywords: Universal calibration; Fractal calibration; Organic gel packings; Calibration; Polymers

1. Introduction

The size-exclusion chromatography (SEC) mechanism separates polymeric solutes according to their sizes in solution, that is, based only on entropy changes. In this case the elution behaviour is presented in terms of the universal calibration curves made by plotting the hydrodynamic volumes, V_h (as $\log M[\eta]$), versus the elution volumes, V_e [1,2].

However, in real systems, enthalpic interactions between different components (solvent, polymeric solutes and gel packing) accompany the separation process, affecting the corresponding value of the sample elution volume [3]. This behaviour was observed in the past when using interactive columns based in silica gels [4,5] but also even in the case of non-interactive column packings such as those based on a polystyrene–divinylbenzene (PS–DVB) copolymer [6–8], a widely used type of cross-linked material [9].

Deviations of the universal calibration are then observed because while $\log M[\eta]$ represents only the size of the macromolecule due to the solvent and temperature used, the chromatographic parameter V_e depends not only on the size but also on other effects

*Corresponding author. Fax: +34-96-386-4564.
E-mail address: rosa.garcia@uv.es (A. Campos).
[1]Present address: Department of Chemistry, University of Cambridge, Cambridge, UK.

0021-9673/03/$ – see front matter
doi:10.1016/S0021-9673(03)00609-5

through the global distribution coefficient, K_D. In this sense, K_D is the product of the distribution coefficient of size, K_{SEC}, by the distribution coefficient for secondary mechanisms, K_p, mainly representing the effect of binary and ternary solvent–polymer–gel interactions. In other words, V_e represents both size and interactions, so that different values of the elution volumes for the same solute size are expected due to the different strength of the involved interactions. In this regard, the experimental elution data for some of the systems here studied were recently analyzed for other purposes such as to derive an expression to calculate K_p as a function of the thermodynamic g_{ij} interaction functions for a solvent(1)–polymer(2)–gel(3) ternary system [8,10]; to calculate the crosslinking and swelling degrees of gels [10]; to evaluate the preferential solvation parameter [8,11] and to study the concentration effects on the elution volumes [11].

On the other hand, it is known that the porous gel material used as packing in SEC possess a fractal geometry that can be characterized by means of the fractal dimension, D_f, which measures the roughness of a porous surface [12–16]. In this sense, there have been recently some attempts to mathematically modelize the separation of polymers in porous particles when both SEC and hydrodynamic chromatography (HDC) modes are present in the retention mechanism [17]. Moreover, another approach have shown the fractal properties of some alumino-silicate supports for metal catalysts by means of the SEC technique [18].

In this work it is shown that, for organic packings, D_f depends both on the geometrical characteristics of the pore and on the heterogeneity of the porous surface, leading to a strong enhancement of polymer–surface interactions, such as reversible adsorption, when the surface irregularity increases [19].

The main goal of the present paper is to propose a relationship between D_f and K_D, which is independent of the chemical nature of the solvent, polymer and gel involved in the chromatographic system. The proposed fractal calibration has been proved to work well, at least when size-exclusion is the main separation mechanism and adsorption a secondary one. However, for other chromatographic modes such as ''critical chromatography'' or ''liquid adsorption chromatography'', where adsorption is not a secondary process, the method has not already been tested.

2. Theory

Size-exclusion chromatography (SEC) is a widely used technique for the analysis and characterization of polymers in solution. The main separation mechanism of the macromolecular solutes is basically based on their sizes, which are reflected by their retention or elution volumes, V_e, independently of the gel packing used provided that the separation process is ''*ideal*'' SEC. In such cases, the Universal Calibration (UC) method proposed by Benoit and coworkers is accomplished and the solute separation follows the well-known relationship [1,2]:

$$\log M[\eta] = a' + b'V_e \quad (1)$$

where the product of molar mass and intrinsic viscosity, $M[\eta]$, represents the solute hydrodynamic volume, V_h, or a size parameter.

However, some drawbacks are encountered under real conditions due to the existence of phenomena different from pure (or ideal) exclusion, i.e., when secondary mechanisms are also present in the separation process. In these cases, the UC method given by Eq. (1) is no longer valid and deviations from a unique calibration curve appear [4,20–27]. In general, the experimentally observed deviations from a single curve depend on the strength and type of the interactions taking place between the different components of the chromatographic system (solvent, polymeric solute and gel packing).

On one hand, the elution volumes are described by:

$$V_e = V_0 + K_D V_p \quad (2)$$

where V_0 and V_p are the interstitial and pore volumes, respectively, of the column, and K_D is a global distribution coefficient that represents the ratio of the solute concentration in the stationary and in the mobile phases. This coefficient takes into account not only the pure exclusion mechanism but also secondary effects, being usually expressed as:

$$K_D = K_{SEC}K_p \quad (3)$$

where the distribution coefficient by size, K_{SEC}, is a thermodynamic parameter defined as [28]:

$$K_{SEC} = \exp(\Delta S/R) \quad (4)$$

and reflects the change in the conformational entropy, ΔS, when the macromolecule is transferred from the mobile phase to the inside of the stationary phase (gel). Since the conformational degrees of freedom of a macromolecule are more restricted inside the pores of the packing, the entropy always decreases during permeation into the pores, and as result $\Delta S<0$ and $K_{SEC}<1$.

Regarding to the distribution coefficient that accounts for secondary mechanisms, K_p, it is thermodynamically defined as [29]:

$$K_p = \exp(-\Delta H/RT) \quad (5)$$

and represents the enthalpy change, ΔH, of the separation process as a consequence of the different binary and ternary interactions between solvent, polymer and gel. When repulsive polymer–gel interactions occur, $\Delta H>0$ and $K_p<1$, whereas attractive interactions, such as reversible adsorption of the solute onto the gel surface, yield an $\Delta H<0$ and $K_p>1$.

On the other hand, it is well-known that the size parameter $M[\eta]$ given in Eq. (1) is related to the mean quadratic end-to-end distance, $\langle r^2\rangle$, by the Flory–Fox model:

$$M[\eta] = \Phi\langle r^2\rangle^{3/2} \quad (6)$$

where Φ is the Flory universal constant. Note that this equation is only an approximation since the Flory's so-called universal constant is not such a constant. Firstly, there are at least a dozen of different values in the literature; and, secondly, it must to have into account the quality of the solvent and the dependence of the polymer molar mass. Nevertheless, this equation is not used for quantitative calculations in the present work, we only pretend to evidence that the hydrodynamic volume, $M[\eta]$, is a measure of the macromolecular size.

Therefore, on the light of Eqs. (2)–(6), it is clearly pointed out that while the $M[\eta]$ parameter is exclusively related to the size of the macromolecule (or entropic effects), the V_e also takes into account the enthalpic effect due to solvent–polymer–gel interactions. Consequently, it is reasonably expected that the same value of $M[\eta]$ yield different values of V_e, depending on such interactions. Therefore, shiftings from the UC curve should be obtained depending on the chemical nature of the chromatographic system and the gel packing used.

Recently, we have shown [10] that the different thermodynamic interaction functions, g_{ij}, are related to the crosslinking degree (chain density per volume unit) and to the swelling degree of the chromatographic supports. In this sense, the crosslinking degree has been related to the entropic contribution to V_e, whereas the swelling degree was associated with the enthalpic effect.

Moreover, in order to understand more-in-depth the UC deviations and find out a unique universal relationship for real chromatographic systems, we think that both the crosslinking and the swelling degrees should be related to the porous roughness of the gel, which can be quantitatively described by the fractal dimension, D_f. In this regard, as suggested by Brochard and co-workers [12,13], porous materials such as those used in SEC can be considered as surface fractals. The coefficient K_D has been related to the fractal dimension of the pore surface through [12]:

$$K_D = 1 - \left(\frac{R}{L}\right)^{3-D_f} \quad (7)$$

with L standing for the available linear dimension of pores and R for the radius of the solvated macromolecular solute. Indeed, R is the radius of the equivalent hydrodynamic sphere (in Å) and it can be calculated from the intrinsic viscosity (in ml/g) by the Einstein equation:

$$R^3 = \left(\frac{3\times 10^{23} M[\eta]}{\pi N_A}\right) \quad (8)$$

where N_A is Avogadro's number.

As seen from Eq. (7), we believe that the fractal dimension, D_f, reflects both the size of solutes and their possible solvent–polymer and polymer–gel interactions, and therefore, D_f it should be a better parameter than $M[\eta]$ for a SEC calibration plot. This fractal parameter is easily calculated for a given solvent(1)–polymer(2)–gel(3) ternary system from experimental elution and viscosity data, taking natural logarithms in Eq. (7), that is [30]:

$$\ln R = \frac{1}{3 - D_f} \ln(1 - K_D) + \ln L \quad (9)$$

By plotting $\ln R$ versus $\ln(1-K_D)$, a linear relationship is obtained. The slope and intercept allow, respectively, to determine the fractal characteristics of the gel surface and the available pore size. It should be expected that the experimental D_f values range between 2 and 3, that is, between the natural limits for a flat surface or planar geometry ($D_f = 2$) and a three-dimensional one ($D_f = 3$). Moreover, and chromatographically speaking, $D_f \rightarrow 3$ when $K_D \rightarrow 0$ and $D_f \rightarrow 2$ when $K_D \rightarrow 1$.

3. Experimental

3.1. Chemicals

Narrow standard polymer samples of polybutadiene (PBD) purchased from Polymer Source (Dorval, Canada); poly(dimethylsiloxane) (PDMS) from Polymer Laboratories (Shropshire, UK) and Polymer Source; polystyrene (PS) from Polymer Standard Service-USA (MD, USA) and Pressure Chemical (PA, USA); and poly(methylmethacrylate) (PMMA) from Polymer Laboratories have been used in the present work. Their average molar masses, M_w, polydispersity index and those samples used with the different gel packings are compiled in Table 1.

Tetrahydrofuran (THF), benzene (Bz), toluene (Tol), 1–4 dioxane (Diox) and cyclohexane (CHX) of chromatographic grade from Scharlau (Barcelona, Spain) were used as solvents or eluents.

3.2. Chromatography

A Waters liquid chromatography equipment with refractive index detector used for SEC experiments have been recently described [31–33]. Three sets of columns (each one of 7.8 mm I.D.×300 mm) based on a PS–DVB copolymer and with the following characteristics have been used: (i) three μ-styragel columns from Waters (Mildford, MA, USA); (ii) three TSK Gel H_{HR} from Tosohaas, Tosoh (Tokyo, Japan); and (iii) three TSK Gel H_{XL} from Tosohaas. Their packing characteristics as particle size, nominal pore size, pore and total exclusion volumes (V_p and V_0) and molar mass separation range are gathered in Table 2. All the solvents used as eluents

Table 1
Weight-average molar masses ($\overline{M}_w$) of the narrow standard polymers used for the SEC measurements in each column packing

$\overline{M}_w$ (g mol^{-1})						
PS[a,b,c]	PBD[a]	PBD[b]	PBD[c]	PDMS[a,b]	PDMS[c]	PMMA[c]
4136	5950	5950	920	8100	1140	5780
6870	13 400	13 400	6250	41 500	8100	26 900
17 200	67 300	47 000	12 600	76 030	33 500	70 500
30 000	87 000	67 300	34 000	188 400	123 000	160 500
42 000	268 000	87 000	60 700	681 600	188 000	254 700
90 100	1 120 000	94 250	105 700			550 000
114 000		268 000	323 000			
207 750		1 120 000	360 000			
355 000						
400 000						
657 000						
1 432 000						
2 700 000						
3 800 000						

Polydispersity index: PS (1.05–1.10); PBD (1.03–1.15); PDMS (1.06–1.23); PMMA (1.03–1.15).
[a] Used in μ-styragel.
[b] Used in TSK Gel H_{HR}.
[c] Used in TSK Gel H_{XL}.

Table 2
Column packing characteristics

Commercial name	Gel packing	Pore size	Particle size (μm)	Effective M_w range	V_0 (ml)[a]	V_p (ml)	V_T (ml)[b]
μ-Styragel	Copolymer PS–DVB	10^3 Å	15	200–30 000	17.7	18.1	35.8
		10^4 Å		5000–600 000			
		10^5 Å		50 000–4 Million			
TSK Gel H_{HR}	Copolymer PS–DVB	G 2500	5	200–40 000	16.4	21.0	37.4
		G 4000		1000–600 000			
		G 6000		10 000–4 Million			
TSK Gel H_{XL}	Copolymer PS–DVB	G 2500	5	200–40 000	17.07	16.63	33.7
		G 4000	6	1000–600 000			
		G 6000	9	10 000–4 Million			

[a] Determined with a PS standard of high molar mass ($M_w = 3\,800\,000$).
[b] Determined with small molecules as THF, Tol or Bz.

were previously degassed and filtered by passing them under vacuum through a 0.45-μm regenerated cellulose filter from Micro Filtration Systems (Dublin, CA, USA). All chromatographic experiments were performed at 25 °C in a thermostated heater and the columns were equilibrated overnight prior to starting any experiment. Chromatograms were obtained at a flow-rate of 1.0 ml min^{-1} by injection of 100 μl of sample solution. To avoid concentration effects [6] on the elution volumes, V_e, all solute samples were injected at four concentrations and then extrapolated to zero concentration. The elution behaviour has been presented in terms of the ''universal calibration'' curves made by plotting the hydrodynamic volumes, V_h (as $\log M[\eta]$) versus V_e, and fitted using only the linear region of the curve (with $r^2 \geq 0.997$).

3.3. Viscometric measurements

The intrinsic viscosity, $[\eta]$, of each sample in a given solvent was calculated according to the Mark–Houwink–Sakurada (MHS) equation: $[\eta] = KM^{\boldsymbol{a}}$. The values of the MHS parameters, K and $\boldsymbol{a}$, for all the systems studied are listed in Table 3 and were determined by measuring the specific viscosities at 25 °C as previously described [10].

4. Results and discussion

4.1. Chromatographic behaviour

The experimental elution data were plotted according to Eq. (1) and the major part of them have been recently published in a review for the three packings assayed [34]. The values of the elution volumes, V_e, were extrapolated to zero concentration ($c \rightarrow 0$) since they are affected by different factors such as the injected solute concentration, the thermodynamic quality of the solvent [35–38], the viscous fingering [39], and the preferential sorption [11], among others. According to Eq. (1), a linear relationship is obtained in all cases, being the values of the inter-

Table 3
Viscometric data (MHS parameters) at 25 °C for binary solvent–polymer systems (from Ref. [10])

System	K (ml g^{-1})	$\boldsymbol{a}$
THF–PBD	0.0109	0.760
Bz–PBD	0.1120	0.604
Diox–PBD	0.1550	0.541
Bz–PDMS	0.0579	0.572
Tol–PDMS	0.0447	0.601
CHX–PDMS	0.1590	0.534
THF–PS	0.0110	0.725
THF–PMMA	0.0075	0.720
Diox–PMMA	0.0114	0.714

Table 4
Linear fit parameters, a' (intercept) and b' (slope) of Eq. (1) for different systems in the three sets of columns.

System	μ-Styragel		TSK Gel H_{HR}		TSK Gel H_{XL}	
	a'	b' (ml^{-1})	a'	b' (ml^{-1})	a'	b' (ml^{-1})
THF–PBD	16.26	−0.411	18.51	−0.580	17.57	−0.506
Bz–PBD	15.00	−0.333	16.27	−0.451	18.12	−0.477
Diox–PBD	16.62	−0.360	18.79	−0.555	16.10	−0.464
Bz–PDMS	15.50	−0.373	16.77	−0.469	17.16	−0.465
Tol–PDMS	16.80	−0.426	17.88	−0.535	17.24	−0.522
CHX–PDMS	15.80	−0.376	16.85	−0.456	16.23	−0.462
THF–PS	16.12	−0.413	16.73	−0.470	18.24	−0.527
THF–PMMA					18.12	−0.529
Diox–PMMA					18.40	−0.590

cepts and slopes of the corresponding linear fits compiled in Table 4 for all the systems assayed (including new data corresponding to the elution of PMMA in TSK Gel H_{XL}). As it was shown [10,34] and from the values in Table 4, deviations from a unique curve are observed for different solvent–polymer systems in a given gel packing, or even for the same system when eluting in different commercial chromatographic supports. The elution volumes are shifted to lower or higher values than those expected for an ideal size-exclusion separation mechanism when incompatibility or compatibility between solute and gel appears, respectively.

The observed deviations from a single UC curve are, concretely, a consequence of binary interactions between the three components of the system, as can be deduced from Figs. 1 and 2. In these figures we have compared the calibration curves when changing either the type of gel (component 3), or the polymer chemical nature (component 2) or the solvent (component 1) used. In the first case, shiftings may be ascribable to solvent(1)–gel(3) and polymer(2)–gel(3) interactions, whereas in the second case it should be attributed to solvent(1)–polymer(2) and polymer(2)–gel(3) interactions. However, when only the solvent is changed, solvent(1)–polymer(2) and solvent(1)–gel(3) interactions could be responsible of the observed shiftings.

Fig. 1 plots the comparison of different binary systems: THF–PS (part a), THF–PBD (part b) and Tol–PDMS (part c) in the three packings studied. From part a to part c of figure, the chemical nature of the polymeric solute(2) has also been changed, choosing in each case the best solvent for the polymer, i.e., that solvent with better thermodynamic quality given by the highest value of the ***a*** parameter (see values in Table 3). As seen, for THF–PS, the solvent–polymer and solvent–gel interactions are the same since the gels are also based on a polystyrene network. Therefore, the differences on the elution of the solute are only due to the strength of the polymer–gel interactions, which follow the sequence: PS–μ-styragel > PS–TSK Gel H_{XL} > PS–TSK Gel H_{HR}. The same trend is observed for the elution of PBD in THF, whereas in the case of PDMS eluted in Tol, the order in the intensity of the corresponding polymer–gel interaction is: PDMS–μ-styragel > PDMS–TSK Gel H_{HR} > PDMS–TSK Gel H_{XL}. In conclusion, a given solvent–polymer system elutes differently depending on the gel used, which means that the intrinsic and microscopic nature of the gel is the major responsible of the observed behaviour. Since all the selected packings are based on a PS–DVB copolymer, the differences could be mainly attributed to their crosslinking degrees, as we will explain more-in-depth later. However, the enthalpic interactions between the solute and the remaining moieties left as residual surface groups by the manufacturing procedure of gel packings could also be responsible, although in minor extension, of the observed differences.

In Fig. 2, comparisons are made based on a change of solvent for a given gel, specifically, the TSK Gel H_{XL} and a given polymer solute: PBD (part a), PDMS (part b) and PMMA (part c). In consequence, the experimental deviations are mainly due to solvent–gel interactions. As we can see, whatever the polymeric solute is, the higher attractive solvent–

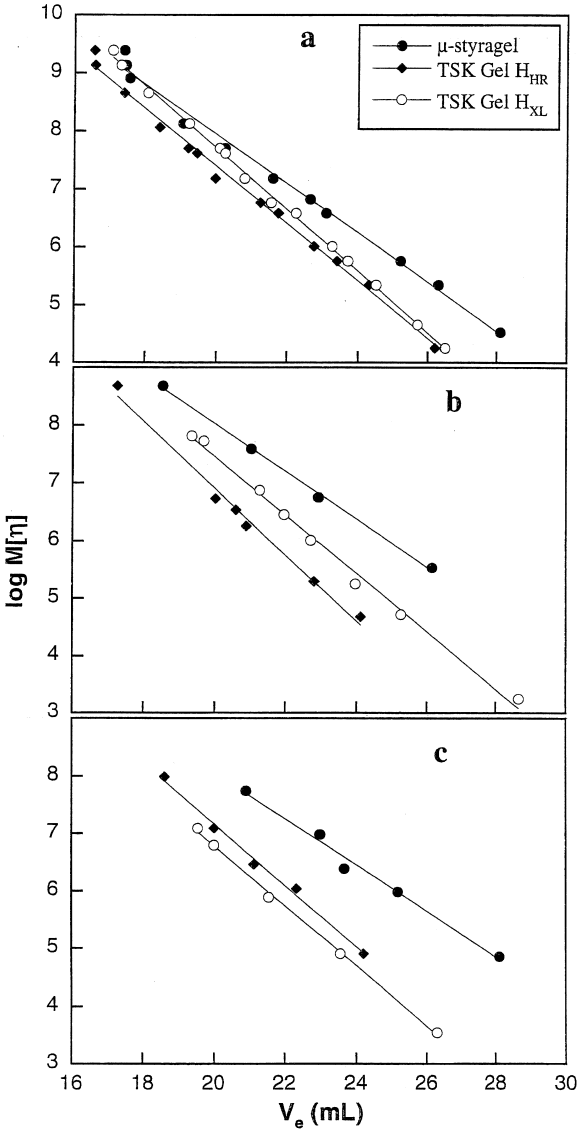

Fig. 1. Comparison of the universal calibration plots, in the three packings studied, for the systems: (a) THF–PS; (b) THF–PBD; and (c) Tol–PDMS.

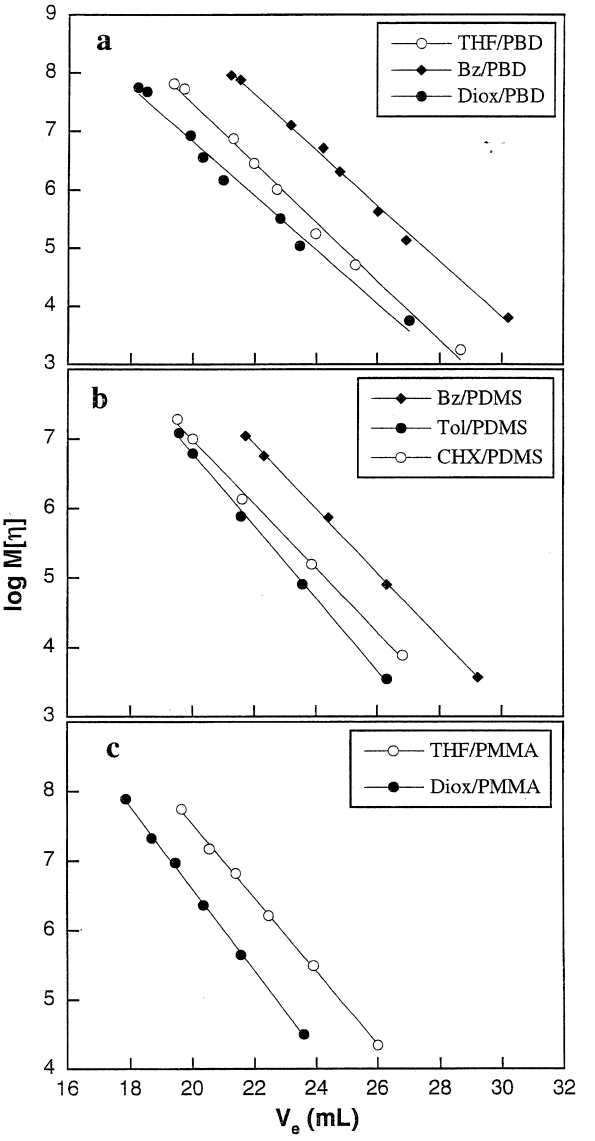

Fig. 2. Comparison of the elution behaviour of different solvent–polymer systems in TSK Gel H$_{XL}$, for the following polymeric solutes: (a) PBD; (b) PDMS; and (c) PMMA.

gel interactions occur for those solvents that possess the lower ***a*** value (see Table 3). Thermodynamically speaking, this means that as the solvent worse solvates the polymer, the affinity of the polymer by the gel packing is favoured, since the binary interactions involved in the ternary system are competitive. Consequently, lower elution volumes are expected and the corresponding calibration curves will be shifted to the left side. This experimental chromatographic behaviour is supported by the corresponding K_p values compiled in Table 5. At any hydrodynamic volume, in TSK Gel H$_{XL}$, the highest value of the distribution coefficient corresponds to the calibration curve more shifted to the right side. Therefore, the PBD solute is more adsorbed onto the gel when eluted in Bz; for PDMS as solute also occurs in Bz,

Table 5
Distribution coefficients for secondary mechanisms, K_p, in the three packings studied at different hydrodynamic volumes selected

System	K_p								
	$V_h = 10^6$ (ml mol^{-1})			$V_h = 10^7$ (ml mol^{-1})			$V_h = 10^8$ (ml mol^{-1})		
	μ-Styragel	TSK Gel H_{HR}	TSK Gel H_{XL}	μ-Styragel	TSK Gel H_{HR}	TSK Gel H_{XL}	μ-Styragel	TSK Gel H_{HR}	TSK Gel H_{XL}
THF–PBD	1.006	0.981	1.307	0.992	0.966	1.515	0.958	0.935	3.013
Bz–PBD	1.293	1.205	1.876	1.298	1.160	2.466	1.325	1.038	6.725
Diox–PBD	1.636	1.265	1.056	1.853	1.364	1.004	2.490	1.659	0.628
Bz–PDMS	1.077	1.246	1.557	1.043	1.244	1.886	0.962	1.243	4.257
Tol–PDMS	1.061	1.097	1.000	1.089	1.095	1.000	1.181	1.103	1.001
CHX–PDMS	1.159	1.408	1.142	1.171	1.462	1.151	1.217	1.638	1.214
THF–PS	0.933	1.215	1.383	0.890	1.216	1.688	0.771	1.233	3.887

The K_p data for μ-styragel and TSK Gel H_{HR} are from Refs. [10,11]. They have been included for the sake of comparison.

and for the case of PMMA in THF. Similar comparisons have been previously made for the other two SEC packings: μ-styragel and TSK Gel H_{HR} [11,34,40]. For the sake of comparison, the corresponding K_p values are also gathered in Table 5.

Summarizing and as evidenced from Figs. 1–2, there is no a unique universal calibration curve when plotting $\log M[\eta]$, a magnitude that only considers the entropic effects, against the elution volumes that account for both entropic (size) and enthalpic factors, which are related through the K_p coefficient to the thermodynamic binary interaction functions, g_{ij}, between the three components of the system [8,10].

4.2. Fractal behaviour

Furthermore, entropic and enthalpic effects are intimately related with the crosslinking and swelling degrees, respectively, of the chromatographic support [10]. And, both packing characteristics can be described by the roughness of the gel surface, or in other words, by the fractal surface that the polymeric solute ''encounters'' when permeating into the pores of the gel. The fractality of the surface is usually represented by its fractal dimension, D_f, and both D_f and V_e are magnitudes representative of the entropic and enthalpic aspects of the chromatographic separation process. In this regard, fractal behaviour evidence was early shown for different solvent–polymer systems eluted in inorganic and active packings silica-based for SEC [41].

For the organic PS–DVB gels here analyzed, the fractal behaviour is also evidenced in Fig. 3 where, as an example, Eq. (9) has been plotted for the system THF–PS in the three type of columns (part a) and for PBD in TSK Gel H_{XL} when changing the

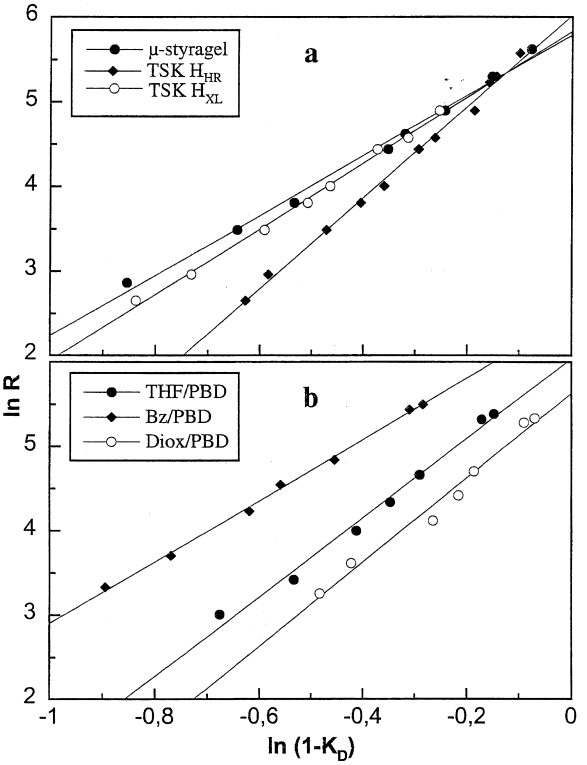

Fig. 3. Plot of Eq. (9) for: (a) THF–PS in the three gel packings assayed; and (b) solvent–PBD systems in TSK Gel H_{XL}.

solvent (part b). Similar plots have been made for the remaining systems but they are not shown here for simplicity. Again, different linear relationships appear when any component of the system (solvent, polymer or gel) is changed, since ln R is a magnitude that exclusively represents the size of the macromolecule in solution. However, Eq. (9) allows the evaluation of the fractal dimension of the gel surface, D_f, and the available pore size, L, from the slopes and intercepts, respectively, of the linear fits. Data of D_f and L values obtained for all the systems, at $V_h = 10^6$ ml mol^{-1}, are compiled in Table 6, together with the values of the global distribution coefficient, K_D. As can be seen, there is a D_f value for each system independently of the molar mass, M, of the polymeric solute since the fractal dimension is a parameter characteristic of the pore surface as swollen by the solvent. Moreover, the lower values reached by D_f correspond to those systems with the worse thermodynamic quality of the solvents (given by their lower $\boldsymbol{a}$ values). Consequently, the gel packing will be less swollen and will exhibit a lower roughness in the pore surface. At a given size (V_h or $M[\eta]$), a dependence of D_f with K_D is observed. Altogether, the D_f values are comprised between the logical limits, that is, 2 and 3, but nearer to 3 denoting a quasi-three-dimensional surface, whereas in rigid gels such as those based on silica, such as Spherosil and Lichrospher, D_f values were substantially lower, approaching to the minimum value of 2 [41]. Moreover, it is worthwhile mentioning that, as D_f increases, the separation efficiency of the SEC columns also does.

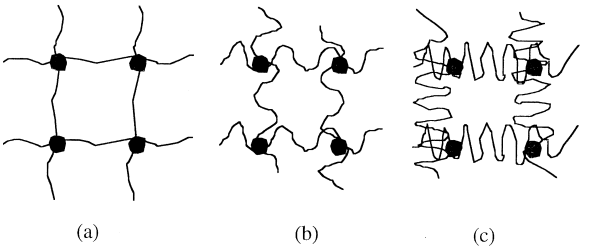

Scheme 1.

In general, the analysis of the D_f values here obtained for each type of column assayed, yields the conclusion that, whatever the system eluted, the fractality of theses surfaces is in the following order: D_f (H_{HR} gel) > D_f (H_{XL} gel) > D_f (μ-styragel).

Regarding the L values, the general tendency follows the same sequence, that is: L (H_{HR} gel) > L (H_{XL} gel) > L (μ-styragel). The behaviour of both magnitudes can be understood taking into account the chemical nature of the gel and, therefore, its network architecture. According to previous work [10,34] and data from the manufacturers [42], the swelling degree of the three gels here studied is in the same order, being the TSK Gel H_{HR} the most swollen by a given solvent, and the μ-styragel the lowest, as illustrated by Scheme 1. In this schematic figure, picture (a) stands for μ-styragel, (b) for TSK Gel H_{XL} and (c) for TSK Gel H_{HR}. As can be seen, it could be reasonably pointed out that as the swelling degree increases, the void volume will decrease (given that the total volume is constant) and, as a

Table 6
Chromatographic distribution coefficients, K_D, and fractal properties, D_f and L, for different polymeric gel packings (Data for $V_h = M[\eta] = 10^6$ ml mol^{-1})

System	μ-Styragel			TSK Gel H_{HR}			TSK Gel H_{XL}		
	K_D	D_f	L (Å)	K_D	D_f	L (Å)	K_D	D_f	L (Å)
THF–PBD	0.405	2.73	403	0.246	2.86	446	0.350	2.79	420
Bz–PBD	0.521	2.63	428	0.302	2.84	507	0.501	2.72	686
Diox–PBD	0.659	2.49	509	0.317	2.84	648	0.282	2.80	278
Bz–PDMS	0.434	2.66	317	0.313	2.81	430	0.416	2.70	356
Tol–PDMS	0.427	2.71	400	0.275	2.84	455	0.267	2.80	266
CHX–PDMS	0.463	2.67	395	0.353	2.80	513	0.305	2.77	273
THF–PS	0.379	2.74	408	0.307	2.83	528	0.370	2.78	497
THF–PMMA							0.350	2.77	375
Diox–PMMA							0.238	2.83	276

consequence, both the fractal dimension of the surface and the available pore size could also increase.

Another interesting analysis of the D_f values consists on the comparison in a given polymer–gel system when changing the solvent. For example, in μ-styragel and PBD as solute, we observed that D_f (THF)>D_f (Bz)>D_f (Diox), which is in agreement with the thermodynamic quality or ''goodness'' (see Table 3) of these solvents to swell the gel and to increase the roughness of the pore surface. Therefore, Scheme 1 can also apply to this situation, being now picture (a) representative for Diox, (b) for Bz and (c) for THF, as solvents.

Finally, the D_f and K_D values compiled in Table 6 for 23 systems have been plotted in Fig. 4, at constant hydrodynamic volume ($V_h = M[\eta] = 10^6$). As can be seen, we have found a linear relationship between D_f and K_D independent of either the chemical nature of the solvent–polymer system eluted or the type of gel. A similar linearity was found when choosing other different values of V_h (not shown here for simplicity). The linear fit of Fig. 4 plot have resulted to be: $D_f = 3.070 - 0.857K_D$ (with $r^2 = 0.96$), which, although empirical, is in perfect agreement with the expected from theoretical considerations, i.e., that for $K_D = 0$, $D_f \to 3$ and when $K_D = 1$, $D_f \to 2$.

All these findings lead us to propose a ''fractal calibration'' curve by plotting D_f versus K_D (at constant V_h), being both magnitudes simultaneously representative of the entropic and enthalpic effects (or size + interactions) accounting in a SEC chromatographic process.

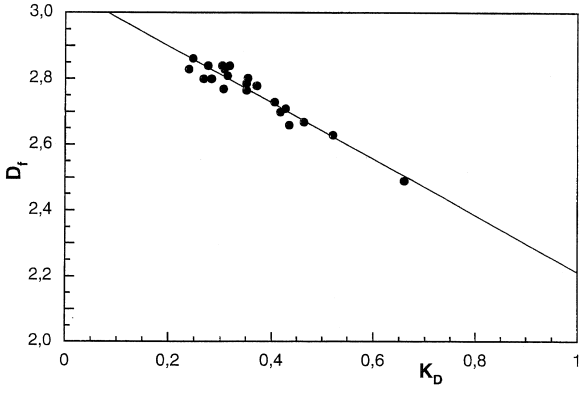

Fig. 4. Fractal calibration plot for all the systems eluted in the three type of columns, at $V_h = 10^6$ ml mol^{-1}.

The main advantage of the proposed fractal calibration lies in its usefulness and applicability to obtain with a much more low error than with the conventional procedure, the weight average molar mass, $\overline{M}_w$; the number average molar mass, $\overline{M}_n$; the polydispersity index ($\overline{M}_w/\overline{M}_n$), as well as the molar mass distribution of a polymer, that is, to correctly characterize an unknown polymer sample by SEC. To support it, work in this sense is currently in progress, where data from the manufacturers will be compared with those obtained with the classical UC and with the here proposed fractal calibration (in preparation). Moreover, we are trying to generalize the fractal calibration to any hydrodynamic volume in order to complete its applications.

5. Conclusions

The experimental chromatographic data of several solvent–polymer systems eluted in three types of organic column packings for SEC have revealed that the classical universal calibration ($\log M[\eta]$ versus V_e) is not fulfilled. The observed deviations are a consequence of two effects: entropic (ideal size-exclusion) and enthalpic (interactions between solvent, polymer and gel). The understanding of both effects has been based on the gel swelling and crosslinking degrees, and also on the fractal characteristics of the corresponding porous surfaces.

The fractal dimension, D_f, ranges between 2.6 and 2.9 for the columns here tested, that is, near the upper limit of 3 (three-dimensional space) which denotes a high separation efficiency of these supports. Independently of the chemical nature of the solvent–polymer systems eluted, the fractality of the three columns follows the sequence: D_f (TSK Gel H_{HR})>D_f (TSK Gel H_{XL})>D_f (μ-styragel). Moreover, the same trend has been obtained for the real pore size: L (TSK Gel H_{HR})>L (TSK Gel H_{XL})>L (μ-styragel). These tendencies are also in agreement with the network architecture of the assayed gels, showing that the highest the swelling degree (or the lowest the network crosslinking) the highest the fractal dimension and the highest the available pore size.

The global analysis of data has allowed us to propose a relationship between the fractal dimension, D_f, and the chromatographic distribution coefficient, K_D, both representing simultaneously the entropic and the enthalpic effects. This alternative fractal calibration is independent of the chemical nature of the solvent, polymer and gel, and provides us with a potential and useful tool to characterize with very low error polymer unknown samples.

Acknowledgements

Financial support from Ministerio de Ciencia y Tecnología (Spain) under Grant No. MAT2000-1781 is gratefully acknowledged. One of us (I.I.) also thanks to Consejo Nacional de Investigaciones Científicas y Técnicas (CONICET) and to the Universidad de Buenos Aires (UBA) (Argentina).

References

[1] H. Benoit, Z. Grubisic, P. Rempp, D. Decker, J.G. Zilliox, J. Chim. Phys. 63 (1966) 1507.
[2] Z. Grubisic, P. Rempp, H. Benoit, J. Polym. Sci. Polym. Lett. 5 (1967) 753.
[3] S. Mori, H.G. Barth, in: Size Exclusion Chromatography, Springer, Berlin, 1999.
[4] A. Campos, V. Soria, J.E. Figueruelo, Makromol. Chem. 180 (1979) 1961.
[5] J.E. Figueruelo, A. Campos, V. Soria, Makromol. Chem. 182 (1981) 1525.
[6] D. Berek, in: Column Handbook for Size Exclusion Chromatography, Academic Press, London, 1999, pp. 445–457, Chapter 15.
[7] C.M. Gómez, R. García, J.E. Figueruelo, A. Campos, Macromol. Chem. Phys. 201 (2000) 2354.
[8] R. García, C.M. Gómez, J.E. Figueruelo, A. Campos, Macromol. Chem. Phys. 202 (2001) 1889.
[9] Cross-linked Polymers: Chemistry, Properties and Applications, in: R.A. Dickie, S.S. Labana, R.S. Bauer (Eds.), American Chemical Society Symp. Ser. 367, 1998.
[10] R. García, I.B. Recalde, J.E. Figueruelo, A. Campos, Macromol. Chem. Phys. 202 (2001) 3352.
[11] R. García-Lopera, C.M. Gómez, C. Abad, A. Campos, Macromol. Chem. Phys. 203 (2002) 2551.
[12] F. Brochard, J. Phys. 46 (1985) 2117.
[13] F. Brochard, A. Ghazi, M. Le Maire, M. Martin, Chromatographia 27 (1989) 257.
[14] E. Eisenriegler, in: Polymers near Surfaces, World Scientific, Singapore, 1993.
[15] G.J. Fleer et al., in: Polymers at Interfaces, Chapman & Hall, London, 1993.
[16] T. Garel, H. Orland, Phys. Rev. B 55 (1997) 226.
[17] Y.C. Guillaume, J.F. Robert, C. Guinchard, Anal. Chem. 73 (2001) 3059.
[18] D. Duca, G. Deganello, J. Mol. Catal. A Chem. 112 (1996) 413.
[19] G. Huber, T.A. Vilgis, Eur. Phys. J. B 3 (1998) 217.
[20] D. Bakos, T. Bleha, A. Ozima, D. Berek, J. Appl. Polym. Sci. 23 (1979) 2233.
[21] B.G. Belenkii, L.Z. Vilenchik, in: Modern Liquid Chromatography of Macromolecules, Elsevier, Amsterdam, 1983.
[22] R. García, I. Porcar, A. Campos, V. Soria, J.E. Figueruelo, J. Chromatogr. A 655 (1993) 191.
[23] A. Campos, R. García, I. Porcar, V. Soria, J. Liq. Chromatogr. 17 (1994) 3261.
[24] G. Shah, P.L. Dubin, J. Chromatogr. A 693 (1995) 197.
[25] R. García, I. Porcar, J.E. Figueruelo, V. Soria, A. Campos, J. Chromatogr. A 721 (1996) 203.
[26] D. Berek, M. Janco, G.R. Meira, J. Polym. Sci. Part A: Polym. Chem. 36 (1998) 1363.
[27] M.K. Kosmas, E.P. Bokaris, E.G. Georgaka, Polymer 39 (1998) 4973.
[28] W.W. Yau, J.J. Kirkland, D.D. Bly, in: Modern Size Exclusion Chromatography, Wiley, New York, 1979.
[29] J.V. Dawkins, M. Hemming, Makromol. Chem. 176 (1975) 1795.
[30] M. Le Maire, A. Ghazi, M. Martin, F. Brochard, J. Biochem. 106 (1989) 814.
[31] A. Campos, C.M. Gómez, R. García, J.E. Figueruelo, V. Soria, Polymer 37 (1996) 3361.
[32] C.M. Gómez, J.E. Figueruelo, A. Campos, Polymer 39 (1998) 4023.
[33] C.M. Gómez, J.E. Figueruelo, A. Campos, Macromol. Chem. Phys. 200 (1999) 246.
[34] R. García, C.M. Gómez, A. Codoñer, C. Abad, A. Campos, J. Biochem. Biophys. Methods 1689 (2003) 1.
[35] Y. Kato, T. Hashimoto, J. Appl. Polym. Sci. 18 (1974) 1239.
[36] T. Bleha, D. Bakos, D. Berek, Polymer 18 (1977) 897.
[37] A. Campos, L. Borque, J.E. Figueruelo, Anal. Quím. 74 (1978) 701.
[38] J.E. Figueruelo, A. Campos, V. Soria, R. Tejero, J. Liq. Chromatogr. 7 (1984) 1061.
[39] J. Janca, J. Chromatogr. 134 (1977) 263.
[40] P. Verdú, B.Sc. Project, University of Valencia, Spain, 2001.
[41] I. Porcar, R. García, V. Soria, A. Campos, J.E. Figueruelo, J. Non-Cryst. Solids 147/148 (1992) 170.
[42] Column Catalogues Millipore-Waters and Teknokroma (1999–2000).